

# Luminosity Measurement Method for LHC:

## The theoretical precision and the experimental challenges<sup>\*</sup>

**M. W. Krasny<sup>a,b</sup>, J. Chwastowski<sup>b</sup>, K. Słowikowski<sup>c</sup>**

<sup>a</sup>*LPNHE, Pierre and Marie Curie University, Tour 33, RdC,  
4, pl. Jussieu 75005 Paris, France.*

<sup>b</sup>*Institute of Nuclear Physics HNINP-PAS,  
ul. Radzikowskiego 152, 31-342 Cracow, Poland.*

<sup>c</sup>*Faculty of Physics and Applied Computer Science,  
AGH-University of Sciences and Technology,  
Al. Mickiewicza 30, 30-059 Cracow, Poland.*

### Abstract

This is the first of the series of papers which present a precision method of the day-by-day monitoring of the absolute LHC luminosity. This method is based on the measurement of the rate of coplanar lepton pairs produced in peripheral collisions of the beams' particles. In the present paper we evaluate the modeling precision of the lepton pair production processes in proton-proton collisions, optimize the measurement region to achieve better than 1% accuracy of the predicted rates, and discuss the experimental challenges to filter out the luminosity monitoring lepton pairs at LHC.

---

<sup>\*</sup>The work is supported by the program of cooperation between the IN2P3 and Polish Laboratories No. 05-117 and by the POLONIUM program No. 11580PE.

# 1 Introduction

The Large Hadron Collider (LHC) experimental program is mainly focused on the study of collisions of point-like constituents of the LHC beam particles. If their collision rates could be unambiguously expressed in terms of the scale-dependent, universal partonic luminosities and process-specific cross sections then the measurement of the parent beam luminosity would be of residual importance for such a program. However, the unfolding of partonic luminosities involves modeling of the confinement effects of virtual bunches of partons and the effects of strongly interacting medium which neither can be controlled by the perturbative QCD nor can be proved to be collision-energy independent. Because of these facts the only precise, model independent method of the absolute normalisation of the rates of partonic collisions must remain to be based on the measured luminosities of the parent beam particles: protons and ions.

Numerous methods of the LHC luminosity measurement have been proposed - see [1] and references quoted therein for a comprehensible review. In general, all the proposed luminosity measurement methods are based on:

1. the measured properties of the colliding beams: the beam currents and profiles. These methods provide the luminosity delivered to the interaction point and need to be corrected for the dead-time of the trigger and the data acquisition systems to determine the recorded luminosity. The expected accuracy of such methods is of the order of 10% [2],
2. a simultaneous measurement of the rate of two processes inter-linked via the optical theorem. These methods can be applied only in the dedicated collider runs with high  $\beta^*$  beam optics. The luminosity measurement must be subsequently extrapolated to the standard low  $\beta^*$  ones. The expected measurement accuracy in the high  $\beta^*$  mode is 2-3% [3]. The precision of the extrapolation will depend upon the machine operating conditions and, at present, cannot be reliably estimated,
3. the measurement of the rates of the electromagnetic processes. The precision of these methods is in the range of 2-5%. It reflects the process dependent resolving power of the internal charge structure of the beam particles. Several methods minimizing the impact of the internal charge structure of the colliding particles have been elaborated by the HERA collider experiments [4], and could be used at LHC.
4. a dedicated machine runs with hybrid beams [6]. In these runs a parasitic electron beam carried to the interaction point by the ions could be used for the measurement of the absolute machine luminosity. A precision of 1-2% similar to that of the HERA collider [4, 5] can be achieved.

The discussion of the methods belonging to each of these four categories is beyond the scope of this paper. This and the subsequent papers document an attempt to select the method which, in our view, has the largest potential of providing the highest precision at the LHC, and to develop a proposal of the complete **luminosity measurement procedure** which includes: high-precision modeling of the signal and background processes, the proposals of the dedicated detector and the trigger, construction of the on- and off-line data selection and the data-monitoring algorithms, and last, but not least, elaboration of the concrete luminosity counting methods.

Our primary goal is to achieve a  $\leq 1\%$  statistical, theoretical and systematic precision of the absolute normalisation of the collected event samples on a daily basis, and to provide handy tools for measuring the cross sections for any user selected event sample, regardless of their sampling frequency and the luminosity-block-based data segmentation. Moreover, our aim is to provide dedicated tools for a high precision on-line monitoring of the bunch-by-bunch relative luminosity at the time granularity of a couple of seconds for an efficient machine operation feedback. Last but not the least, our goal is to develop a method which is universal for any beam species colliding at the LHC, protons and ions. This last point is particularly important for a high precision scrutinizing of the polarisation asymmetry in the collisions of effective beams of polarised W-bosons with hadronic matter discussed in [7].

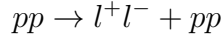
It is obvious that the highest precision of the luminosity measurement for the colliding beams of strongly interacting composite particles could be achieved by counting the rate of their highly peripheral collisions. In such collisions the internal structure of the beam particles and their strong interactions may be neglected. Thus, their rate can be precisely calculated using exclusively the QED perturbative methods. It can be expressed solely in terms of the static properties of the beam particles: their masses, electric charges and magnetic moments - the parameters which are known to a very high precision [8].

The simplest “luminometric” process which could satisfy the above condition is the small angle, elastic scattering of the beam particles. However, for the high luminosity (small  $\beta^*$ ) operation mode of the ring-ring colliders the highly-peripheral, elastic collisions cannot be efficiently selected. A remedy, elaborated and employed successfully at HERA, was to select the process of quasi-elastic *radiative scattering*

$$ep \rightarrow e + \gamma + p$$

and use the radiative photon as the collision peripherality tagger. Only a fraction of radiative photons can play such a role. In the HERA collider case the photon must be emitted co-linearly to the incoming electron (the bremsstrahlung process [9]) or its transverse momentum must balance the electron transverse momentum (the Compton process [10]).

An equivalent process for hadronic colliders is the quasi-elastic lepton pair production process



in which the lepton pair is emitted co-linearly to the beams' collision axis. The luminosity measurement method presented in this and subsequent papers employs such pairs for the tagging of peripheral processes at LHC in the same manner as the radiative photons were employed at HERA. The above analogy enables us to make use of our experience gained at HERA [4, 5] while developing a proposal of the luminosity measurement procedure for LHC. Apart from the differences in the detection schemes of the photons and of the lepton pairs the measurement procedure will essentially remain the same as that developed and tested at HERA.

This paper is the first of the series of papers presenting such a proposal. It is organized as follows. In section 2 we describe the experimental signatures and the modeling of the lepton pair production processes. We concentrate on the proton–proton case leaving the discussion of the ion–proton and ion–ion collisions to a dedicated paper [11]. In section 3 we discuss the optimisation of the measurement region to achieve the highest statistical and theoretical precision of the predicted event rates. In section 4 we present the experimental challenges which the measurement of the rate of lepton pair production in the selected phase-space region must face.

## 2 Lepton pair production at LHC

### 2.1 Phase-space region selection

Budnev, Ginzburg, Meledin and Serbo [13] were first to propose the lepton pair production process for a precise determination of the proton–proton collision luminosity at high energy colliders.

This process has already been studied as a candidate process to measure luminosity at LHC. Production of electron–positron pairs in the central pseudorapidity region was studied by Telnov [14]. These studies were abandoned because of a lack of a viable triggering scheme for such pairs.

The detection of forward-produced  $e^+e^-$  pairs with a very small invariant mass,  $M_{ll} \leq 0.01\text{GeV}$ , at the distance of 19 m from the LHC interaction point, was proposed in [15] and [16]. The measurement in this phase-space region is difficult because of the limited experimental means of controlling the beam–beam and beam–wall (beam–gas) collision background. In addition, such a measurement requires not only a precise mapping of the magnetic field and the dead material over the distance of 19 meters, but also a precise knowledge of the beam angular divergence. Last but not the least, the event rates in this kinematic region are sensitive to bunch

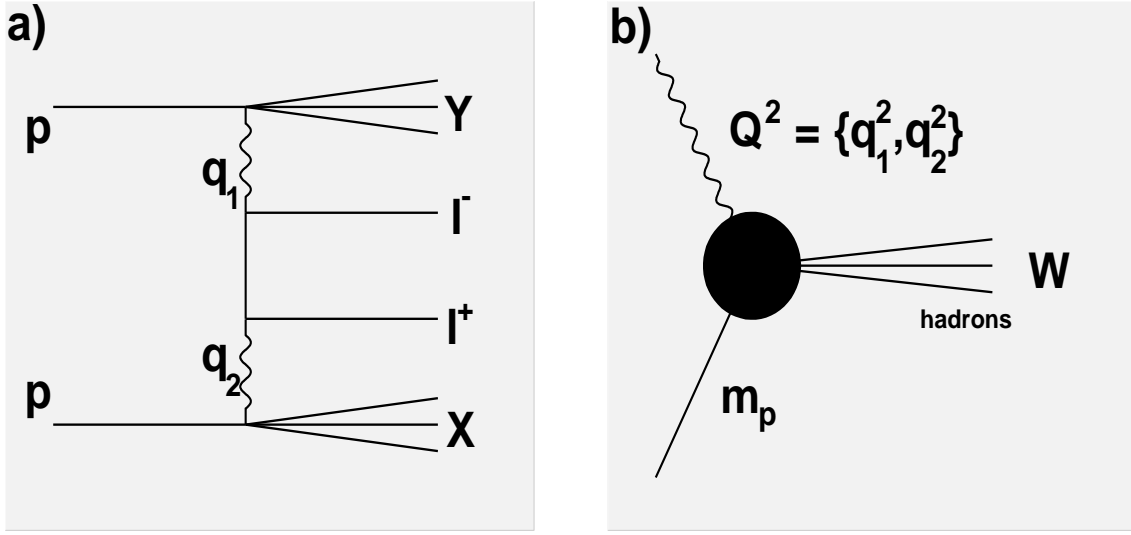


Figure 1: (a) Electromagnetic production of lepton pairs in proton–proton collision. X and Y represent either the remnants of the protons produced in inelastic collisions or the outgoing protons for the elastic ones, (b) the vertex of the electromagnetic probe of the proton structure.

dynamics, in particular to the space-charge effects of the LHC bunches. This method has also been abandoned.

Production of muon pairs in the central pseudorapidity region, proposed first by A. Courau [17], has been studied in [18]. The authors of [18] argued that this process could be used to determine the LHC luminosity with  $\sim 2\%$  systematic precision. To achieve such a precision the machine and the beam-collision background must, however, be small enough to allow for an efficient triggering of muons down to the transverse momenta of  $p_t^\mu = 6$  GeV/c. The most important limitation of this method is, however, its statistical precision. The cross section for production of the muon pair of high invariant mass is small and 1% statistical precision of the luminosity measurement can be achieved only on the year-by-year, rather than on the day-by-day, basis at the machine luminosity of  $\mathcal{L} = 10^{33} \text{ cm}^{-2} \text{ s}^{-1}$ .

For the method presented here we choose the phase-space region of the invariant mass of the lepton pair  $M_{ll} \geq 0.4$  GeV. We focus our attention on those of the beam collisions in which the lepton pair is produced exclusively in the pseudorapidity region  $-2.7 < \eta < 2.7$ . In the selected region of centrally-produced and a relatively large invariant mass<sup>1</sup> pairs each of the two leptons is produced at sufficiently large

<sup>1</sup>The invariant mass of the lepton pair is 1000 times higher than the electron mass.

transverse momentum to be independent of the coherent bunch-space-charge effects, and to neglect the proton beams' crossing angle and divergence. Moreover, as far as the electron-positron pairs are concerned, the Dalitz pair background is suppressed. Since the strong interactions of colliding protons are attenuated at the distance scales larger than the typical distance scales of strong interactions:  $1/m_\pi, 1/\Lambda$ , the highly peripheral lepton pairs ( $p_t^{pair} \ll 1/m_\pi, 1/\Lambda$ ) are produced essentially in electromagnetic processes.

The residual contribution of strong interaction processes is further reduced by demanding the presence of rapidity gaps between the lepton pair and the remnants of the incident protons. Such a requirement assures not only the direct electromagnetic coupling of leptons to protons but removes simultaneously the processes in which the lepton pair comes from the decays of produced hadrons. Finally, the choice of centrally produced pairs removes the contribution of radiative lepton pair production by the beam particles and by their low mass excitations originating from the Pomeron mediated collisions.

For the lepton pairs satisfying the above requirements the photon–photon fusion, shown in Fig. 1a, is the dominant Born-level process. The higher order corrections can be classified as the strong interaction and the electromagnetic radiative corrections. The former have been discussed in [1] and were found to be negligible for the the low  $p_t$  lepton pairs. The latter are small [13] and can be controlled at the LHC energies with precision better than 0.1% [19].

## 2.2 Modeling of the lepton pair production processes

### 2.2.1 The LPAIR generator

The LPAIR event generator [20] was used to simulate the lepton pair production events. It is based on a computation by J.A.M. Vermaseren [21]. This is an extension of an earlier work on the lepton pair production in  $e^+e^-$  collisions by P. Kessler [22] and includes, as an option, the formalism for collisions of composite beam particles with an arbitrary charge structure.

In the LPAIR generator the lepton pair production cross section is calculated as a convolution of the fluxes of virtual photons and the cross section for virtual photon collisions:

$$\sigma(p_1, p_2) = \sigma_{\gamma^*\gamma^*\rightarrow l_1 l_2}(p_1, p_2, q_1, q_2) \otimes flux_{\gamma^*}(q_1) \otimes flux_{\gamma^*}(q_2), \quad (1)$$

where  $p_1$  and  $p_2$  represent the four-momenta of the outgoing, on-shell leptons, and  $q_1$  and  $q_2$  the four-momenta of virtual photons. In our analysis we use both the LPAIR matrix element for the  $\gamma^*\gamma^*$  collisions and the LPAIR algorithm for the convolution of the corresponding cross section with virtual photon fluxes. However, we have upgraded the photon flux modeling. Such an upgrade was indispensable

since, as we shall discuss in the following sections, the calculation precision of the event rates was mainly limited by approximations used in the photon flux modeling rather than by the accuracy of the theoretical calculations and the precision of numerical algorithms. It allowed us to study the effects which were neglected in earlier analyses.

### 2.2.2 Photon fluxes

The coupling of a virtual photon to a proton, shown in Fig. 1b, is specified in terms of the proton mass,  $m_p$ , the produced hadronic system mass,  $W = \sqrt{(\Sigma p_i)^2}$ , where  $p_i$  are the four-momenta of all outgoing hadrons, and the four-momentum transfer squared,  $Q^2$ . These Lorenz-invariant variables provide a complete description of the photon–proton coupling for inclusive processes in which the corresponding cross section is integrated over all possible hadronic configurations and summed over the polarisation states of virtual photons. In order to model the photon–proton coupling we split the  $(Q^2, W)$  plane into five regions: the elastic region in which  $W = m_p$ , the resonance region defined by the condition  $m_p + m_\pi \leq W \leq 1.8$  GeV, the photoproduction region satisfying the condition  $Q^2 \leq 0.01$  GeV $^2$ , the deep inelastic region in which  $Q^2 \geq 4$  GeV $^2$ , and the transition region spread over the remaining part of the  $(Q^2, W)$  plane. These regions are shown schematically in Fig. 2.

In the elastic region the photon fluxes are specified in terms of the form factors  $G_E(Q^2)$  and  $G_M(Q^2)$  which have been re-measured at SLAC [23]. In the resonance region we use the parameterised form [24] of the DESY low energy data for the photo-absorption cross section of longitudinally and transversely polarised photons. In the photoproduction and the transition regions we use the parameterisation of [25]. This parameterisation interpolates the data between the photoproduction and the deep inelastic regions and assures a smooth transition to the resonance region. In the deep inelastic region we use the MRS [26] parameterisation of the partonic distribution functions.

## 2.3 Modeling precision

The precision of the LPAIR predictions for the lepton pair rates depends on the matrix element calculation accuracy, the size of the higher order corrections to the process shown in Fig.1a, and the modeling accuracy of the virtual photon fluxes. For the luminosity measurement method discussed in this paper the accuracy of photon flux modeling determines entirely the precision of the predicted lepton pair rates. If ordered according to the increasing modeling precision the lepton pair production processes can be grouped into four classes:

1. the inelastic processes sensitive to the momentum distributions of quarks in the proton (a  $\sim 5\%$  precision),

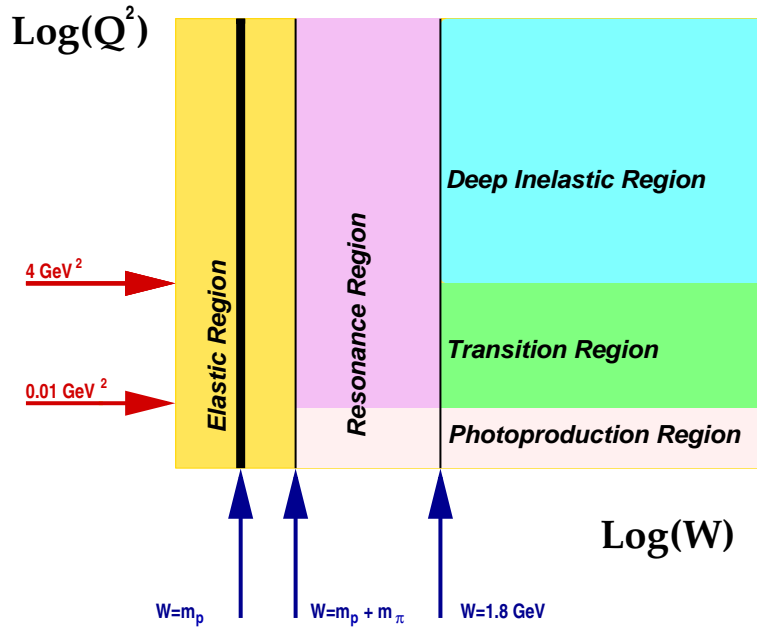


Figure 2: The kinematic regions used in the modeling of the photon fluxes.

2. the inelastic processes sensitive to the collective excitations of quarks in the proton (a  $\sim 4\%$  precision),
3. the elastic processes sensitive to the proton magnetic and electric form factors (a  $\sim 2\%$  precision),
4. the elastic processes in which proton behaves as point-like particle; sensitive only to the proton mass, charge and anomalous magnetic moment which are known to a very high accuracy [8].

In general each of the above classes of processes will contribute to the observed event rate. The goal of the optimisation procedure discussed in the next section is to restrict the phase-space region and to propose the corresponding event selection criteria which maximize the contribution of the elastic “point-like” processes (4). Asymptotically, if the processes (1-3) were totally removed then the luminosity measurement based on the corresponding event sample could be as precise as the luminosity measurement at the  $e^+e^-$  colliders using the Bhabha process [27]. Note that if uncertainty due to contribution of processes (1-3) could be reduced below  $\sim 0.5\%$  of the total rate, the precision of the matrix element calculation would need to be improved (e.g. by creating a new event generator using e.g. the helicity amplitude formalism developed by P. Kessler [22] and including the electromagnetic radiative corrections).

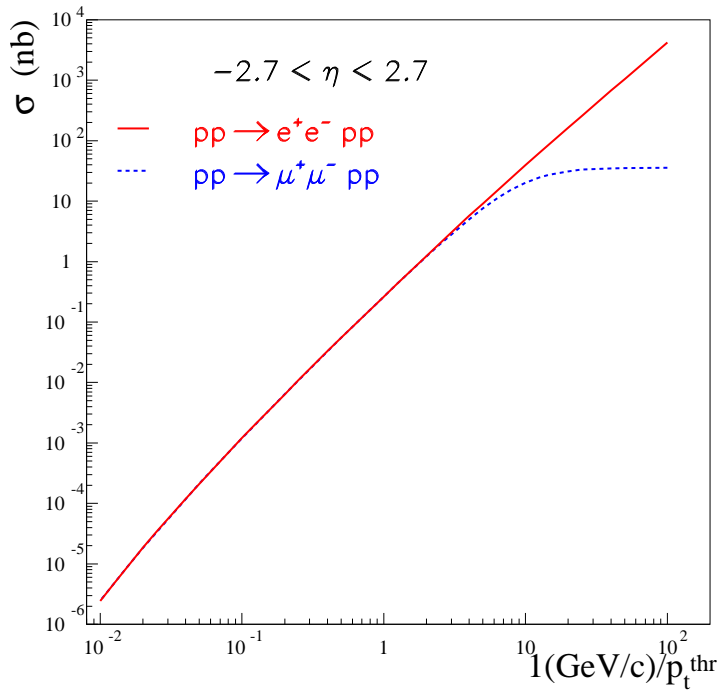


Figure 3: The cross section  $\sigma$  for the lepton pair production in elastic processes plotted as a function  $1(\text{GeV}/c)/p_t^{\text{thr}}$  for the sample of events in which the transverse momenta of both leptons are larger than the transverse momentum threshold,  $p_t^{\text{thr}}$ . The solid line represents the  $e^+e^-$  sample while the  $\mu^+\mu^-$  sample is represented by the dotted line.

## 2.4 Modeling of the background processes

The Pythia event generator [28] was used to develop the methods of the background suppression strategy. The processes which could give rise to the lepton pair signatures are the soft hadronic processes. They have been studied at lower collision energies. Since their extrapolation to the LHC energy domain is highly uncertain, therefore any precision method of the LHC luminosity measurement must not depend upon their modeling. The Pythia generator is used in our studies merely to define the background subtraction strategy and for an initial estimate of the performance requirements for the trigger and data selection methods. The background subtraction strategy, discussed in details in the subsequent paper [12], will be independent of the Monte Carlo modeling of hadronic background processes. The background rates will be determined using the dedicated monitoring data samples collected during the standard LHC runs.

## 3 Optimisation of the measurement region

### 3.1 Statistical precision

In Fig. 3 we show the cross section for the elastic production of the muon and electron pairs in the pseudorapidity region  $-2.7 < \eta < 2.7$ , as a function of the inverse of the lepton transverse momentum detection threshold  $1(\text{GeV}/c)/p_t^{thr}$ . In the kinematic region studied in this paper,  $p_t^{thr} \geq m_\mu$ , the rates of the muon and electron pairs become identical. As a consequence the optimisation of the kinematic domain presented below is lepton flavor invariant.

The cross section strongly depends on the lepton transverse momentum threshold. In order to achieve the statistical accuracy of 1% on daily basis, for the average machine luminosity of  $\mathcal{L} = 10^{33} \text{ cm}^{-2}\text{s}^{-1}$ , events with the lepton transverse momenta down to the value of  $\sim 500 \text{ MeV}/c$  must be efficiently selected. Increasing the lepton  $p_t$ -detection threshold by one order of magnitude reduces the event rate by three orders of magnitude. In such a restricted region 1% statistical precision could be reached only for a one-year-integrated luminosity.

### 3.2 Event samples

In this section we compare the precision of the theoretical control of the lepton pair production rates for the two  $p_t^l$  detection thresholds:  $p_t^{thr1} = 0.2 \text{ GeV}/c$  and  $p_t^{thr2} = 6 \text{ GeV}/c$ . The corresponding samples of the LPAIR generated events will be referred to as the “**central-track-trigger**” (CTT) and the “**high-pt-trigger**” (HPT) samples.

The HPT sample can be collected at LHC by each of the general purpose detectors in the muon channel assuming an optimal performance of the trigger and the on-line event selection systems. The  $p_t^l$  cut is chosen to be the same as in the analysis presented in [18]. On the other hand, the CTT event sample could be collected only if an upgrade of the existing detectors and their triggers is made.

In order to asses the modeling precision of the absolute rates in the selected above kinematic regions we present in Figs. 4a,b the probability density distribution of the  $\log(Q^2/M_p^2)$  variable, for the CTT and HPT samples. The elastic process, as expected, populates the low  $Q^2$  region while the inelastic processes (including: the resonance, the photoproduction and the deep inelastic scattering contributions) dominate at large  $Q^2$ . For the CTT sample (Fig. 4a) the ratio of the elastic to the inelastic contribution is significantly larger than that for the HPT sample (Fig. 4b).

This is a direct consequence of the fact that the elastic plateau, reflecting in the logarithmic scale the  $dQ^2/Q^2$ -shape of the equivalent photon flux and the strongly peaking invariant mass spectrum of the lepton pair, is extended to lower  $Q^2$  values for the CTT sample. This effect is driven by the  $p_t^{thr}$  cut which determines the low

energy cut-off of the spectrum of photons and consequently lowers the minimal  $Q^2$  value for the CTT sample.

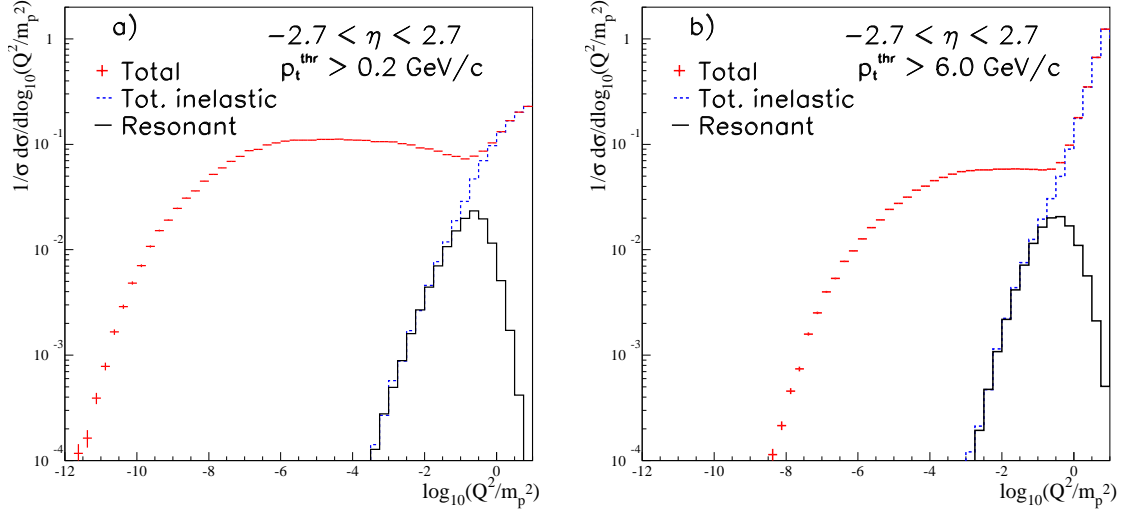


Figure 4: The probability density of the  $\log(Q^2/m_p^2)$  variable, where  $Q^2$  are the four-momentum transfer in the proton vertices and  $m_p$  is the proton mass. The sum of all contributions is represented by crosses. The sum of all inelastic contributions is shown by line dotted line, while the contribution of the low-mass resonant excitations of the proton are represented by the solid line, The distributions are shown separately for the CTT (a) and for the HPT (b) samples. Both leptons are produced in the pseudorapidity region  $-2.7 < \eta < 2.7$

### 3.3 Reduction of modeling uncertainties

The goal of the kinematic domain optimisation, presented below, is to maximize the precision of the theoretical control of the rates while preserving high statistical precision of the day-by-day luminosity. To achieve this goal the contribution of the processes which are sensitive to the internal proton structure must be drastically reduced.

An efficient kinematic variable which was used to control the contribution of the inelastic processes to large angle photon radiation at HERA [4] was the photon-electron acoplanarity. For LHC, where the lepton pair is playing the role of the peripherality tagger the corresponding variable is the lepton pair acoplanarity  $\delta\phi$ . It is defined as  $\delta\phi = \pi - \min(2\pi - |\phi_1 - \phi_2|, |\phi_1 - \phi_2|)$  where  $\phi_1$  and  $\phi_2$  are the

azimuthal angles of produced leptons. The acoplanarity variable is correlated with the transverse momentum of the lepton pair  $p_t^{pair}$ . Since the latter variable is, in turn, strongly correlated with the impact parameter of the colliding protons, the small acoplanarity pairs originate predominantly from the large impact parameter collisions. This region is hardly accessible to the strong interaction processes because of their restricted interaction range. For the small acoplanarity pairs the inelastic excitation of protons in electromagnetic processes is also suppressed due to the QED gauge-invariance which forces the disappearance of the photon coupling to inelastic excitations of protons in the limit of decreasing photon transverse momentum. Because of the above effects the production rate of coplanar pairs in processes which resolve the proton electric and colour charge structure is drastically reduced<sup>2</sup>.

In Fig. 5 we present the acoplanarity distributions for the CTT (5a) and for the HPT (5b) samples and the corresponding  $Q^2$  distribution for the leptons pairs satisfying the conditions  $\delta\phi/\pi \leq 0.01$ , (5c) and (5d). The acoplanarity distribution for the CTT sample is strongly peaked at  $\delta\phi/\pi \simeq 0$  for elastic events and flat for inelastic ones. As expected, the acoplanarity cut removes efficiently the inelastic events. The acoplanarity distribution for the HPT sample is peaked at low acoplanarity both for the elastic and inelastic events. Even if a large fraction of inelastic events is removed by the  $\delta\phi/\pi \leq 0.01$  cut, as shown in Fig. 5d, their remaining contribution, comparable to the elastic one, remains.

In order to achieve better than 1% precision of the theoretical control of the event rates we require the contribution of all inelastic processes to be reduced below the level of 20% of the elastic event rate, and the contribution of those of elastic processes which are sensitive to the proton elastic form factors, to be reduced below the level of 50% of the hypothetical “point-like” event rate. The “point-like” rate is defined here as the pair production rate for a beam of spin 1/2, point-like particles having the mass, the charge, and the anomalous magnetic moment of the proton. It can be calculated with precision limited only by the theoretical precision of the matrix element  $\gamma^*\gamma^* \rightarrow l^+l^-$  and its higher order corrections.

In Fig. 6a we show the ratios of the total pair-production cross section to the elastic cross section for the CTT (solid line) and for the HPT (dotted line) samples as a function of the upper limit of the accepted acoplanarity of a pair. For the CTT sample, already for a loose  $\delta\phi/\pi \leq 0.1$  cut, the contribution of the inelastic processes is ten times smaller than of the elastic one. For the HPT sample an equivalent acoplanarity cut which reduces the contribution of inelastic processes below 20% of the elastic one is  $\delta\phi/\pi \leq 0.002$ . Note that the asymptotic behaviour of the ratios at small acoplanarities reflects the difference in the lepton transverse

---

<sup>2</sup>Note, that, in general, the large  $Q^2$  value is not necessarily correlated with large transverse momentum of the lepton pair. This correlation becomes strong only for the processes in which the energy transfer from the proton to the virtual photon is significantly smaller than the initial proton momentum.

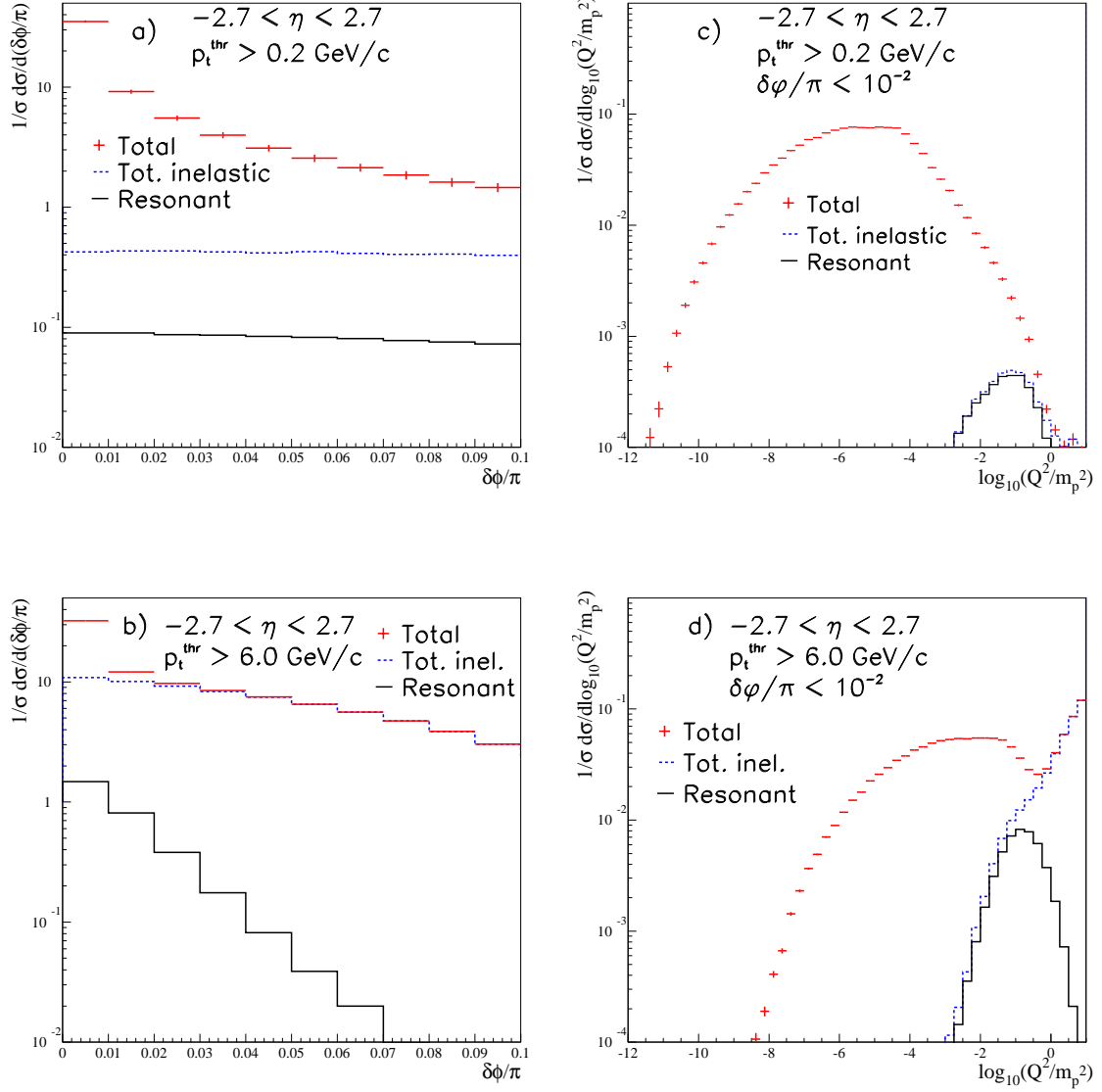


Figure 5: The acoplanarity distribution for lepton pairs produced in the pseudorapidity range:  $-2.7 < \eta < 2.7$  for the CTT (a) and the HPT (b) samples. The distribution of the logarithm of the four-momentum transfer squared,  $\log(Q^2/m_p^2)$ , for events satisfying the condition  $\delta\phi/\pi \leq 0.01$  for the CTT (c) and for the HPT (d) samples. The sum of all contributions is represented by crosses, the sum of inelastic contributions is shown by dotted line, and the resonance contribution by solid line.

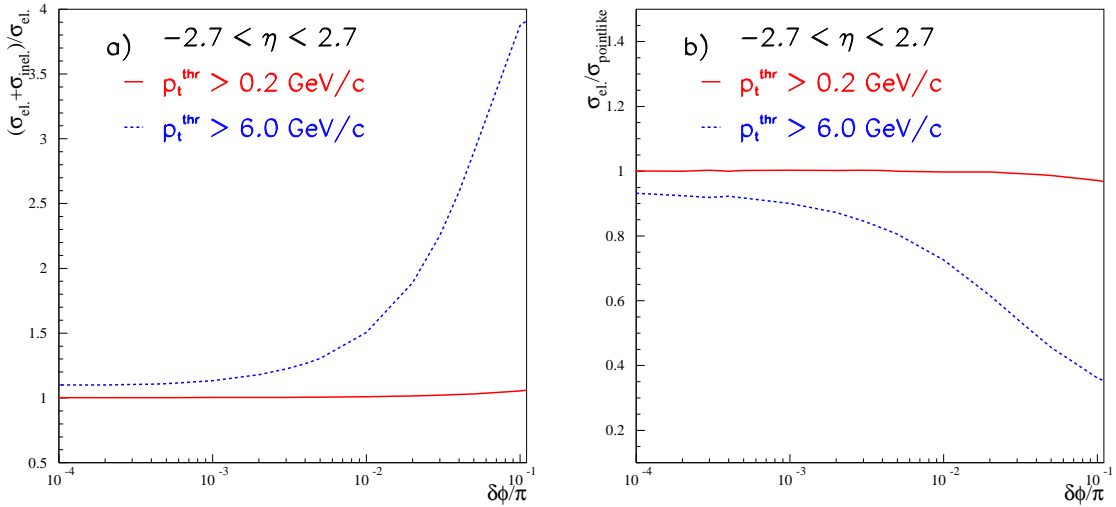


Figure 6: The ratio of the total cross section for the lepton pair production to the elastic one for the CTT (solid line) and the HPT (dotted line) samples as a function of the upper limit on the lepton pair acoplanarity (a). The ratio of the elastic cross section for the lepton pair production to the “point-like” one for the CTT (solid line) and the HPT (dotted line) samples as a function of the upper limit on the lepton pair acoplanarity (b).

momentum cuts for the CTT and HPT sample. For the same acoplanarity larger transverse momenta of the lepton pairs are accepted for the latter sample.

In Fig. 6b we show the ratios of the elastic section to the “point-like” cross section for the CTT (solid line) and for the HPT (dotted line) samples as a function of the upper limit of the acoplanarity of a pair. For the CTT sample, the contribution to the elastic cross section sensitive to the proton form factors stays below 20% of the “point-like” cross section regardless of the acoplanarity cut. For the HPT sample, the contribution to the elastic cross section, sensitive to the proton form factors, is reduced below the required value of 50% only if the initial event sample is restricted to a subsample of events satisfying the condition:  $\delta\phi/\pi \leq 0.03$ . Note that in the case of the HPT sample the decrease of the elastic contribution at high  $Q^2$  values is driven by the proton elastic form factors while for the CTT sample by the  $p_t^{\text{thr}} = 0.2 \text{ GeV}/c$  cut. The latter cut effectively reduces the contribution of the elastic processes in which the proton dipole structure is resolved. It is responsible for faster convergence, of the CTT sample ratio to the value of one with decreasing acoplanarity.

The statistical accuracy of predicted event rate decreases if the acoplanarity range is restricted. This effect is very weak down to the acoplanarities of  $\delta\phi/\pi \leq 0.1$  but becomes significant for  $\delta\phi/\pi \leq 0.002$  leading to a decrease of the rate of the HPT events by a factor of  $\sim 4$ .

### 3.4 Constraints

We have shown in the previous chapter that for both the CTT and the HPT samples the contributions of processes sensitive to the internal structure of the beam particles can be reduced to a level which assures better than 1% precision of the theoretical control of their rate. However, the luminosity measurement based on the HPT sample is vulnerable to several effects which would, very likely, reduce its final precision. The more restrictive acoplanarity cut would require a significantly better understanding of the resolution tails and biases of the reconstructed azimuthal angles of produced lepton pairs for the HPT sample with respect for the CTT sample. The corresponding reduction of the event rate would extend to, at least, one year the integration time of rates in order to achieve a statistical precision comparable to the theoretical one at  $\mathcal{L} = 10^{33} \text{ cm}^{-2}\text{s}^{-1}$ . The integration time would very likely have to be extended even further if the trigger efficiency for the leptons produced close to the  $p_t = 6 \text{ GeV}/c$  detection threshold would turn out to be low, or if the first-level trigger rate for the hadronic events satisfying the lepton pair selection criteria would be higher than  $\sim 10 \text{ kHz}$ . The latter condition excludes a precise luminosity measurement using the HPT electron pairs [16] and puts a stringent constraint on the maximal acceptable rate of muons coming from the pion and kaon decays. The rate gain at the high luminosity  $\mathcal{L} = 10^{34} \text{ cm}^{-2}\text{s}^{-1}$  may lead to a decrease rather than to an increase of the statistical precision because the trigger would have to couple with faster increase of the background rate with respect to signal one<sup>3</sup>.

For the luminosity measurement using the CTT sample there is no “brick-wall” limit of the reachable theoretical accuracy. The contribution of the inelastic and the elastic, form factor dependent, processes can be reduced further without reducing the signal event rate. A large cross section for this sample, allowing to collect  $10^6$  events over the period of one year of running at  $\mathcal{L} = 10^{33} \text{ cm}^{-2}\text{s}^{-1}$ , would assure not only short luminosity sampling intervals but, more importantly, a precise control of the measurement systematic errors. The increasing systematic precision could be matched by increasing precision of the matrix element calculation for “point-like” processes which is controlled entirely by the cut-off of its perturbative expansion. As the example of the LEP experiments has shown, a significantly better precision of the luminosity measurements was achieved than had initially been anticipated.

---

<sup>3</sup>The significance of the above problems could be diminished if the first level trigger of the LHC experiments would be upgraded from the object-multiplicity scheme to the object topology scheme. Such an upgrade is, to our best knowledge, presently not planned.

This is the main reason that we shall concentrate in this and subsequent papers only on the luminosity measurement method based on the CTT sample being, in our view, the method which could ultimately provide the highest precision for the absolute normalisation of the LHC measurements.

At present none of the LHC experiments has the capacity to trigger the CTT events and to filter them out with required efficiency. In order to select these events an upgrade of the existing detectors is indispensable. Any upgrade proposal will have to face not only the challenges specific to the LHC machine environment but also the challenges of its incorporation within the environment of the LHC detectors, which were optimised for precise measurements of the large transverse momentum particles. These experimental challenges facing any upgrade concept are discussed below.

## 4 The experimental challenges

### 4.1 Rejection of strong interaction background

In Fig. 7a we show the rate of the opposite charge particle pairs in the pseudorapidity region  $-2.7 < \eta < 2.7$  as a function of the upper limit of the allowed pair acoplanarity. The rate for the CTT sample (solid line) is compared to the corresponding one for the multi-particle production processes modeled with Pythia (dotted line). All stable, unlike-charge particle pairs produced in the pseudorapidity range  $-2.7 < \eta < 2.7$  with transverse momenta larger than  $0.2 \text{ GeV}/c$  contribute to these rates. This plot illustrates a basic difficulty in selecting the peripheral electromagnetic collisions. For the luminosity of  $\mathcal{L} = 10^{33} \text{ cm}^{-2}s^{-1}$ , the predicted, integrated rate of the signal pairs is at the Hz level while that of the background pairs reaches the GHz level. The challenge is twofold and concerns both the overall rate of background pairs and their efficient rejection. First of all, the design of the dedicated trigger, the on- and off-line data selection method, must assure the overall background pair rejection of nine orders of magnitude. However, the most important challenge is to achieve a sufficiently large suppression of the background rates already at the very early stage of the data selection process - preferentially at the first trigger level operating at large frequency.

### 4.2 Event pile-up

The signal and the background rates shown in Fig. 7a are calculated for continuous beams of colliding particles. In reality, the LHC beams are bunched. For the nominal LHC bunch collision frequency and the nominal luminosity several interactions occur simultaneously within a bunch crossing.

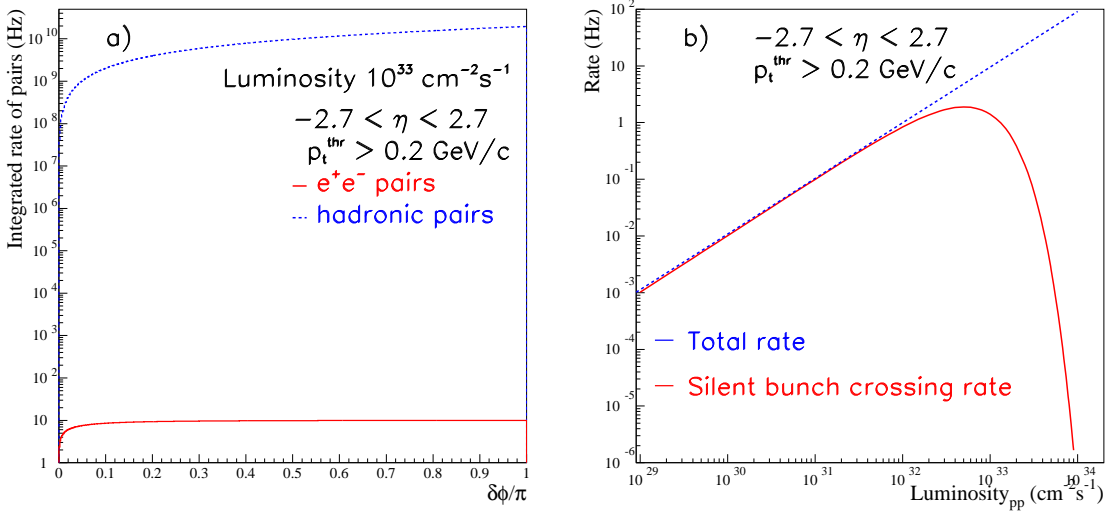


Figure 7: The integrated rate of the charged particle pairs as a function of the acoplanarity angle for the CTT sample (solid line) and the background (Pythia) sample (dotted line) for the luminosity  $\mathcal{L} = 10^{33} \text{ cm}^{-2} \text{s}^{-1}$  (a). The dependence of the CTT event rate on the proton–proton luminosity (b). The “silent bunch crossing” rate (see text for details) is represented by the solid line and the total rate is represented by the dotted line.

In Fig. 7b we show the luminosity dependence of the total integrated rate of the CTT events and the rate of those of CTT events which are produced in the “silent bunch crossings” defined as the bunch crossings with no pile-up hadronic collisions. We assumed  $\sigma_{pp}^{tot} = 79 \text{ mbarn}$  and that the total machine luminosity will be distributed uniformly to all the LHC bunch-crossings occurring with the frequency of 40 MHz. This plot demonstrates that already for the luminosities larger than  $\mathcal{L} \geq 2 \times 10^{31} \text{ cm}^{-2} \text{s}^{-1}$  the lepton pair signal events have a non-negligible probability to overlap with minimum bias interactions.

The challenge specific to the bunched beam is thus to develop the trigger and the on-line selection methods for the CTT lepton pairs which are flexible enough to work in a luminosity-dependent environment of synchronous, minimum bias beam collisions.

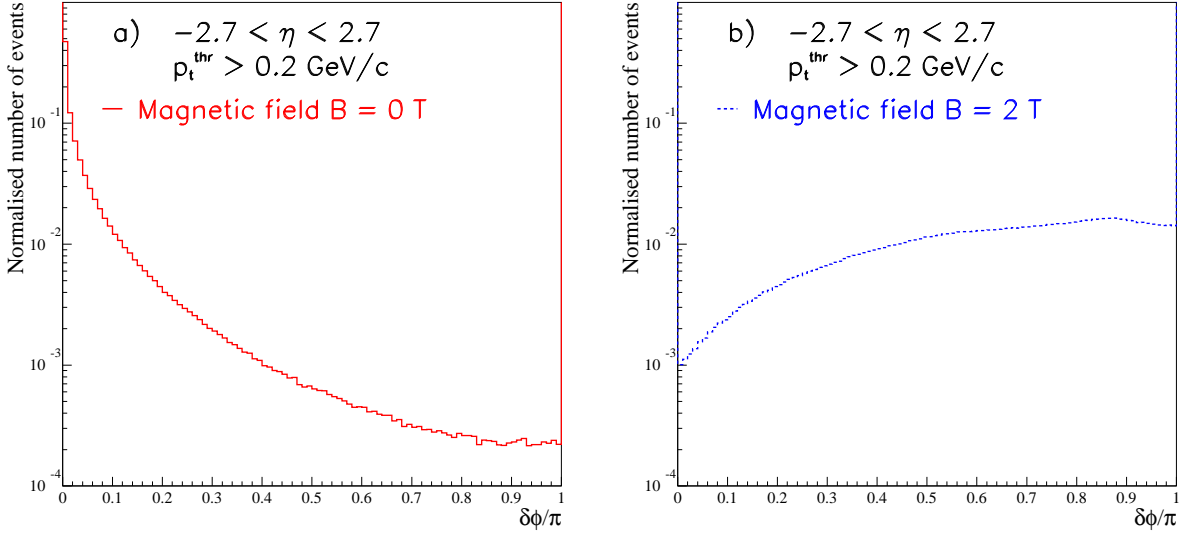


Figure 8: The acoplanarity distribution of the intersection of the lepton trajectories with the  $z = 330$  cm plane perpendicular to the colliding beam axis for the CTT event sample: for  $B = 0$  Tesla (a) , and for  $B = 2$  Tesla (b).

### 4.3 Coplanar lepton pairs in magnetic field

The lepton pairs in the CTT event sample are coplanar. On the other hand, the background pairs coming from strong interaction processes are uniformly distributed over the allowed acoplanarity range. This distinction could be used at the early stage of the event selection process. However, designing an efficient trigger for coplanar, small transverse momenta leptons is by no means straightforward. The standard LHC detector's triggers have been optimized for large energy depositions (electron trigger) and high transverse momentum tracks (muon trigger). Any upgrade project must provide not only the extension of the triggering scheme and use the signatures of small transverse momentum particles but, what is more challenging, it must face the fact that these particles will traverse the region of strong magnetic field.

To illustrate the influence of the magnetic field on the initially-coplanar lepton pairs we show in Fig. 8 the lepton pair acoplanarity distribution on the plane perpendicular to the beam collision axis at the distance of  $z = 286$  cm from the interaction point for the two values of the solenoidal magnetic field of  $B = 0$  and  $B = 2$  Tesla. This plot shows that the magnetic field essentially de-correlates the pair's initial acoplanarity. As a consequence the lepton's hit positions cannot be directly used by the event selection algorithm as the indicator of the initial pair acoplanarity.

Thus, the challenge for triggering the coplanar pairs is to develop a very fast and efficient method of deriving their initial (interaction vertex) acoplanarities from the suitable space-time snapshots of the B-field and lepton pair kinematic dependent acoplanarity evolution.

## 5 Conclusions and outlook

In this paper we have studied the lepton pair production process  $pp \rightarrow l^+l^- + X$  and its merits for the high precision luminosity measurement at the LHC collider. We have selected the kinematic region in which the rate of the lepton pairs produced in peripheral collisions of the beam particles is large enough to achieve a 1% statistical precision of the luminosity measurement on the day-by-day basis. We have demonstrated that better than 1% precision of the theoretical control of the pair rate can be reached by a suitable restriction of the phase-space which suppresses the contribution of the inelastic collisions and those of elastic collisions in which the internal charge-structure of the protons is resolved.

Selecting lepton-pairs in the above phase space region represents a major challenge which, at present, is beyond the reach of the LHC detectors. In the forthcoming paper [12] we shall discuss the necessary detector and the trigger system upgrade to meet this challenge. We shall propose the measurement strategy which aims at achieving a comparable systematic measurement precision to the statical and theoretical ones.

## References

- [1] V. A. Khoze, A. D. Martin, R. Orava and M. G. Ryskin, Luminosity Monitors at the LHC. *Eur. Phys. J.* **C19**, 313 (2001).
- [2] S. van der Meer, Calibration of the Effective Beam Height at the ISR. CERN-ISR-PO **68**, (1968).
- [3] ATLAS Collaboration, ATLAS Forward Detectors for Luminosity Measurement and Monitoring. CERN/LHCC/2004-010 **LHCC I-014**, 123 (2004).
- [4] H1 Collaboration, Experimental Study of Hard Photon Radiation Processes at HERA. *Z. Phys* **C66**, 529 (1995).
- [5] J. Andruszków et al., Luminosity Measurement in the ZEUS Experiment. *Acta Phys. Polon.* **B32**, 2025 (2001).
- [6] M. W. Krasny, Electron Beam for LHC. *Nucl. Instr. Meth.* **A540**, 222 (2005).

- [7] M. W. Krasny, S. Jadach and W. Płaczek, The Femto-experiment for the LHC:  $W$ -boson Beams and Their Targets. *Eur. Phys. J.* **C44**, 333 (2005)
- [8] Particle Data Group, *Eur. Phys. J.* **C15**, 1 (2000)
- [9] L. Suszycki et al., Fast Luminosity Monitoring for HERA. *Nukleonika* **31**, 205 (1986).
- [10] A. Courau and P. Kessler, Detector Calibration, Luminosity Monitoring and Search for an  $e^*$  at HERA. *Phys. Rev.* **D33**, 2028 (1986).
- [11] M. W. Krasny, J. Chwastowski and K. Słowikowski, A Precision Luminosity Measurement Method for LHC: Proton-Ion and Ion-Ion collisions. In preparation.
- [12] M. W. Krasny, J. Chwastowski and K. Słowikowski, A Precision Luminosity Measurement Method for LHC: The Detector Model and the Measurement Procedure. In preparation.
- [13] V. M. Budnev, I. F. Ginzburg, G. V. Meledin and V. G. Serbo, The Process  $pp \rightarrow ppe^+e^-$  and the Possibility of Its Calculation by Means of Quantum Electrodynamics Only. *Nucl. Phys.* **B63**, 519 (1973).
- [14] V. Telnov, On Possibility of Luminosity Measurement in ATLAS Using the Process  $pp \rightarrow pp + e^+e^-$ . ATLAS note **PHYS-94-044** (1994), unpublished.
- [15] K. Piotrzkowski, Proposal for Luminosity Measurement at LHC. ATLAS note **PHYS-96-077** (1996), unpublished. D. Bocian, Luminosity Measurement of  $pp$  Collisions with the Two-Photon Process, PhD thesis (1995), unpublished.
- [16] ATLAS Collaboration, Detector and Physics Performance. Technical Design Report. CERN/LHCC/99-14 **TDR 14**, (1999).
- [17] A. Courau, Luminosity Monitoring of Experiments at  $e^+e^-$ ,  $ep$ ,  $p\bar{p}$  Super Colliders. *Phys. Lett.* **B151**, 469 (1985).
- [18] A. G. Shamov and V. I. Telnov, Precision Luminosity Measurement at LHC Using Two-Photon Production of  $\mu^+\mu^-$  pairs. *Nucl. Instr. Meth.* **A494**, 51 (2002).
- [19] S. Jadach, Private communication.
- [20] S. P. Baranov, O. Dunger, H. Shooshtari and J.A.M. Vermaasen, LPAIR - A Generator for Lepton Pair Production. Proceedings of Physics at HERA, vol. 3, 1478 (1992).

- [21] J. A. M. Vermaseren, Two-Photon Processes At Very High Energies. *Nucl. Phys.* **B229**, 347 (1983).
- [22] P. Kessler. A Generalized Helicity Method for Feynman Diagram Calculations. *Nucl. Phys.* **B15**, 253 (1970).
- [23] E 140 experiment, Measurements of the Proton Elastic Form Factors for  $1 - GeV/c^2 \leq Q^2 \leq 3 - GeV/c^2$  at SLAC. *Phys. Rev.* **D49**, 5671 (1994).
- [24] F.W. Brasse et al., Parameterisation of the  $Q^2$  Dependence of Virtual  $\gamma p$  Total Cross Sections in the Resonance Region. *Nucl. Phys.* **B110**, 413 (1976).
- [25] H. Abramowicz et al., A Parameterisation of  $\sigma_T(\gamma^* p)$  Above the Resonance Region  $Q^2 \geq 0$ . *Phys. Lett.* **B269**, 465 (1991).
- [26] A. D. Martin, R. G. Roberts and W. J. Stirling, MRS (1994): Parton Distributions of the Proton. e-Print Archive: [hep-ph/9409257](https://arxiv.org/abs/hep-ph/9409257)
- [27] S. Jadach, See e.g. “Theoretical Error of Luminosity Cross Section at LEP”. Invited talk at Mini-Workshop on Electroweak Precision Data and the Higgs Mass, Zeuthen, Germany, 28 Feb - 1 Mar 2003.
- [28] T. Sjöstrand, L. Lönnblad and S. Mrenna, PYTHIA 6.2: Physics and manual. e-Print Archive: [hep-ph/0108264](https://arxiv.org/abs/hep-ph/0108264)